



ORIGINAL ARTICLE

Associations between perfusion defects, tissue changes and myocardial deformation in hypertrophic cardiomyopathy, uncovered by a cardiac magnetic resonance segmental analysis

Pedro Garcia Brás^{a,*}, Sílvia Aguiar Rosa^{a,b}, Boban Thomas^b, António Fiarresga^a, Isabel Cardoso^a, Ricardo Pereira^b, Gonçalo Branco^b, Inês Cruz^c, Luís Baquero^b, Rui Cruz Ferreira^a, Miguel Mota Carmo^b, Luís Rocha Lopes^{d,e,f}



^a Department of Cardiology, Santa Marta Hospital, Lisbon, Portugal

^b Heart Center, Red Cross Hospital, Lisbon, Portugal

^c Hospital Garcia de Orta, Almada, Portugal

^d Inherited Cardiac Disease Unit, Bart's Heart Centre, St Bartholomew's Hospital, London, United Kingdom

^e Centre for Heart Muscle Disease, Institute of Cardiovascular Science, University College London, United Kingdom

^f Cardiovascular Centre, University of Lisbon, Portugal

Received 8 March 2022; accepted 22 March 2022

Available online 20 May 2022

KEYWORDS

Hypertrophic cardiomyopathy; Cardiac magnetic resonance; Coronary microvascular dysfunction; Tissue characteristics; Myocardial deformation; Strain imaging

Abstract

Background: Microvascular dysfunction is an often overlooked feature of hypertrophic cardiomyopathy (HCM). Our aim was to assess the association between microvascular dysfunction, wall thickness, tissue characteristics and myocardial deformation in HCM patients, by analyzing individual myocardial segments.

Methods: Prospective assessment including cardiac magnetic resonance to assess wall thickness, T1 and T2 mapping, extracellular volume, late gadolinium enhancement (LGE) and stress perfusion. Results were stratified according to the 16 American Heart Association segments.

Results: Seventy-five patients were recruited (1200 segments), 63% male, mean age 54.6 ± 14.8 years, maximal wall thickness of 20.22 ± 4.6 mm. Among the 424 segments (35%) with perfusion defects, 24% had defects only in the endocardial layer and 12% in both endocardial and epicardial layers. Perfusion defects were more often detected in hypertrophied segments (64%). Among the 660 segments with normal wall thickness, 19% presented perfusion defects. Independently of wall thickness, segments with perfusion defects had a higher T1 (β -estimate 30.28, $p < 0.001$), extracellular volume (β -estimate 1.50, $p < 0.001$) and T2 (β -estimate 0.73, $p < 0.001$) and had late gadolinium enhancement more frequently (odds ratio 4.16, $p < 0.001$). Higher values of circumferential strain (lower deformation) and lower values of radial strain were found in segments with perfusion defects (β -estimate 2.76, $p < 0.001$; and β -estimate -10.39, $p < 0.001$, circumferential and radial strain, respectively).

* Corresponding author.

E-mail address: pedrobras3@gmail.com (P. Garcia Brás).

PALAVRAS-CHAVE

Miocardiopatia hipertrófica; Ressonância magnética cardiovascular; Disfunção coronária microvascular; Características tecidulares; Deformação miocárdica; *Strain imaging*

Conclusion: While microvascular dysfunction was more prevalent in more hypertrophied segments, it also had a major presence in segments without hypertrophy. In this segmental analysis, we found an association between the presence of ischemia and tissue abnormalities, replacement fibrosis as well as impaired strain, independently of the segmental wall thickness.
 © 2022 Sociedade Portuguesa de Cardiologia. Published by Elsevier España, S.L.U. This is an open access article under the CC BY-NC-ND license (<http://creativecommons.org/licenses/by-nc-nd/4.0/>).

Associações entre defeitos de perfusão, características tecidulares e deformação miocárdica na miocardiopatia hipertrófica, uma análise segmentar por ressonância magnética cardíaca

Resumo

Introdução: A disfunção microvascular é uma característica frequentemente subestimada da miocardiopatia hipertrófica (MCH). O objetivo do estudo foi avaliar a associação entre disfunção microvascular, espessura da parede (EP), características tecidulares e deformação miocárdica na MCH, analisando os segmentos miocárdicos individualmente.

Métodos: Estudo prospectivo incluindo ressonância magnética cardíaca para avaliação de EP, T1 e T2 mapping, volume extracelular (VEC), realce tardio (RT) e estudo de perfusão, estratificados de acordo com os 16 segmentos da *American Heart Association*.

Resultados: Foram recrutados 75 doentes (1.200 segmentos), 63% do sexo masculino, idade média $54,6 \pm 14,8$ anos e EP máxima de $20,22 \pm 4,6$ mm. Dentro dos 424 segmentos (35%) com defeitos de perfusão, 24% apresentaram defeitos apenas no endocárdio e 12% apresentaram defeitos tanto no endocárdio como no epicárdio. Os defeitos de perfusão foram detetados maioritariamente nos segmentos hipertrófiados (64%). Dentro dos 660 segmentos com EP normal, 19% apresentaram defeitos de perfusão. Independentemente da EP, os segmentos com defeitos de perfusão apresentaram maior elevação de T1 (β -estimate 30,28, $p < 0,001$), VEC (β -estimate 1,50, $p < 0,001$) e T2 (β -estimate 0,73, $p < 0,001$) e RT com maior frequência (OR 4,16, $p < 0,001$). Os segmentos com defeitos de perfusão apresentaram valores mais elevados de *strain* circunferencial (menor deformação) (β -estimate 2,76, $p < 0,001$) e valores mais reduzidos de *strain* radial (β -estimate -10,39, $p < 0,001$).

Conclusão: Embora a disfunção microvascular tenha sido mais prevalente nos segmentos mais hipertrófiados, esta estava significativamente presente em segmentos sem hipertrófia. Nesta análise segmentar revelamos uma associação entre a presença de isquémia e características tecidulares, fibrose de substituição e *strain* anormal, independentemente da espessura da parede.

© 2022 Sociedade Portuguesa de Cardiologia. Publicado por Elsevier España, S.L.U. Este é um artigo Open Access sob uma licença CC BY-NC-ND (<http://creativecommons.org/licenses/by-nc-nd/4.0/>).

Introduction

Unexplained left ventricular (LV) wall thickening defines hypertrophic cardiomyopathy (HCM)¹ and myocardial fibrosis is a prevalent feature with prognostic relevance.^{2–6} Coronary microvascular dysfunction (CMD) and ischemia have also been identified as playing an important pathophysiological role, linked with replacement fibrosis and, consequently, progressive heart failure, ventricular arrhythmias and sudden cardiac death.^{7–11} Although ischemia is more pronounced in hypertrophied segments,^{12–14} it may be present in non-hypertrophied segments¹⁵ and may even occur before hypertrophy in mutation carriers.¹⁶

Cardiovascular magnetic resonance (CMR) parametric mapping techniques and the calculation of extracellular

volume (ECV) enables more sensitive detection of interstitial fibrosis, with late gadolinium enhancement (LGE) correlating principally with replacement fibrosis.^{3,4,17–20} Abnormalities in native T1 mapping have also been attributed to intracellular abnormalities, such as altered calcium pathways and impaired energy homeostasis.²¹ Increased T2 values have been described in HCM, associated with signs of advanced disease, such as higher LV mass, lower ejection fraction and greater extent of LGE.²²

Previous studies using CMR or positron emission tomography have described a correlation between the global burden of CMD and LV hypertrophy, extent of LGE and higher T1 mapping^{10,23–26} as well as a higher prevalence of clinical manifestations, incidence of atrial fibrillation (AF) and worse outcomes.^{27,28} A limited number of studies have performed a segmental analysis evaluating microvascular

dysfunction and tissue characteristics, LV hypertrophy and LGE.^{24,25}

Our aim was to perform a more comprehensive analysis, integrating myocardial deformation and its correlation, segment-by-segment, with wall thickness, ischemia and LGE. Due to the intra-individual heterogeneity of the LV in HCM, we hypothesized that by comparing individual LV segments instead of a global myocardial evaluation, a more in-depth correlation could be attained, and novel associations revealed.

Methods

Study population

This prospective study enrolled consecutive adult patients with HCM, seen in the dedicated cardiomyopathy clinics of Santa Marta Hospital (n=70) (Lisbon, Portugal) and Garcia de Orta Hospital (n=13) (Almada, Portugal). CMR studies were performed at the Heart Center, Hospital da Cruz Vermelha Portuguesa (Lisbon, Portugal). The diagnosis of HCM was established according to current guidelines.^{1,29} Obstructive HCM was defined according to a peak gradient of ≥ 30 mmHg in the left ventricular outflow tract (LVOT) at rest or after provocation, on echocardiographic assessment. Inclusion criteria, exclusion criteria and clinical evaluation including ECG and echocardiography occurred as previously published by Aguiar Rosa et al.²³

The study followed the principles outlined in the Declaration of Helsinki. The institutional ethics committees approved the study protocol. All patients provided written informed consent.

Cardiac magnetic resonance protocol and analysis

All subjects underwent the same CMR protocol as previously described by Aguiar Rosa et al.²³ In brief, CMR was performed on a 1.5-T magnetic resonance system (Sola, Siemens, Erlangen, Germany). Using compressed sensing-based techniques, cine images in three long-axis planes and sequential short axis slices were acquired. Pre-contrast short axis T1 maps were generated using a Modified Look Locker Inversion (MOLLI) sequence and pre-contrast short axis T2 maps were generated using a single shot balanced steady state free precession acquisition. Stress perfusion 90 seconds after hyperemia was induced by regadenoson (400 mcg bolus) using 0.05 mmol/kg of gadolinium (Gadovist, Bayer Schering Pharma AG, Berlin, Germany). LGE images were acquired 10–15 minutes after intravenous administration of additional 0.15 mmol/kg of gadolinium at end diastole, using a breath-held segmented inversion-recovery steady state free precession sequence after determining the optimal inversion time using a scout sequence.

CMR interpretation was performed using commercially available software (CMR42, Circle Cardiovascular Imaging, Calgary, Alberta, Canada). LV wall thickness, LV mass, end diastolic volume (EDV), end systolic volume (ESV) and LV ejection fraction (EF) were measured from short axis cine images excluding papillary muscles and trabeculations.

For perfusion assessment, the myocardium was divided into 32 subsegments (16 American Heart Association (AHA)

segments subdivided into an endocardial and epicardial layer). Ischemic burden for each patient was calculated as the number of involved sub-segments, assigning 3% of myocardium to each subsegment. Each segment was analyzed for the presence or absence of perfusion defects. Perfusion defects sparing the subendocardium and coincident with LGE were not considered, as subendocardial involvement is mandatory for microvascular dysfunction defects. The LGE was analyzed per-segment basis using a signal threshold versus reference myocardium of ≥ 6 standard deviation.

Three-dimensional longitudinal, circumferential and radial strains were obtained by manually drawing epicardial and endocardial contours on the end diastolic frame of short axis and long-axis images (four-chamber, two-chamber and three-chamber views), using an automatic feature tracking algorithm from cine images.

For each patient, each of the 16 AHA segments was assessed for LV thickness (≤ 11 mm; 12–14 mm; ≥ 15 mm), presence of perfusion defect, T1 mapping, T2 mapping, ECV, presence of LGE, longitudinal strain, radial strain and circumferential strain.

Statistical analysis

Statistical analysis was performed using the Statistical Package for the Social Sciences, V.23.0 for Windows (SPSS). Point estimates and 95% confidence interval (CI) are described for all mean estimates.

Descriptive statistics are presented as absolute frequency (number) and relative frequency (percentage) for categorical variables and as the mean for continuous variables.

The Kolmogorov-Smirnov test was used to test normality assumptions.

A segment-by-segment analysis was performed to assess the correlation between ischemia, LV hypertrophy, tissue characteristics and myocardial deformation parameters, calculated with univariable logistic and linear regressions. Subsequently multivariable analyses, adjusted for potential confounders, were performed. Whenever statistical hypothesis testing was used, a significance level of $\alpha=5\%$ was considered.

Results

Seventy-five patients were enrolled. The general baseline characteristics have been described previously.²³ In summary, 47 (63%) were male, mean age was 54.6 ± 14.8 years; 48 (64%) had asymmetric septal hypertrophy and 22 (29%) had apical hypertrophy. The maximal LV wall thickness was 20.2 ± 4.6 mm.

A total of 1200 segments were analyzed. Stress perfusion and mapping images were interpretable in all segments. LGE images were not interpretable in 16 segments from one patient, due to artifacts. The characteristics of each of the 16 AHA segments are presented in Table 1.

Six hundred and sixty (55%) segments had wall thickness of ≤ 11 mm, 210 (17.5%) segments 12–14 mm, and 330 (27.5%) segments ≥ 15 mm. Wall thickness was greater in the basal and mid septum (AHA segments 2, 3, 8 and 9) (Table 1).

Table 1 Characteristics of each American Heart Association (AHA) segment.

Segments	AHA segments*															
	1	2	3	4	5	6	7	8	9	10	11	12	13	14	15	16
Wall thickness (mm)	13.4±5.2	16.3±4.4	14.7±5.4	10.6±4.2	9.4±2.6	10.6±3.5	11.6±5.6	13.9±5.6	14.6±5.1	11.9±4.9	10.3±3.9	10.9±4.2	11.9±5.7	11.8±5.4	11.2±4.8	11.9±5.6
Presence of perfusion defect, n (%)	16 (21.3)	23 (30.7)	26 (34.7)	15 (20)	9 (12)	6 (8)	24 (32)	32 (42.7)	33 (44)	44 (58.7)	26 (34.7)	17 (22.7)	28 (37.4)	44 (58.7)	48 (64)	33 (44)
T1 mapping (ms)	1011±45.3	1036±44.6	1045±50.2	1046.5±44.9	1029.1±54.2	999±47.3	1007.8±49.5	1030.5±43.2	1044.9±41.8	1033.3±41.4	1020.7±42.2	995.4±50.1	1002.5±55.2	1033.4±48.5	1031.2±43	1018.3±62.9
T2 mapping (ms)	50.36±2.89	49.62±3.07	49.47±3.1	50.51±3.24	49.58±3.89	50.07±2.88	51.32±3.45	50.84±4.0	50.4±2.93	49.95±2.71	49.81±2.82	50.4±3.0	52.11±4.31	51.71±4.1	50.9±3.42	51.35±3.82
Presence of LGE, n (%)	35 (47.3)	51 (68.9)	43 (58.1)	24 (32.4)	25 (33.8)	28 (37.8)	35 (47.3)	50 (67.6)	50 (67.6)	32 (43.2)	27 (36.5)	33 (44.6)	44 (59.5)	51 (68.9)	42 (56.8)	40 (54.1)
Extracellular volume (%)	25.9±5	27.6±5.2	26.8±5.5	26.8±4.2	25.5±4.5	24.6±4	27.1±4.9	27.8±5.1	27.6±4.9	26.4±4.2	25.3±4.3	25.4±4.1	27.8±4.7	28.1±5.9	27.6±6.5	27.3±6.8
Longitudinal Strain (%)	-1.79±9.28	-3.77±6.43	-2.05±7.39	-1.45±9.31	3.27±12.67	4.09±11.3	-5.64±8.33	-4.98±8.2	-4.66±7.34	-2.68±9.01	0.06±15.01	-2.71±13.22	-10.42±5.95	-8.6±5.17	-11.36±5.29	-12.86±4.64
Circumferential strain (%)	-18.41±6.07	-14.71±5.37	-12.66±5.54	-14.16±5.97	-17.8±6.59	-20.55±4.9	-18.98±6.32	-18.88±5.14	-15.71±5.15	-13.61±5.19	-18.05±6.73	-18.0±7.28	-18.16±7.04	-19.43±5.82	-17.28±6.2	-19.55±6.7
Radial strain (%)	23.55±16.93	18.02±13.64	23.98±14.96	31.78±15.55	42.14±24.07	41.97±44.47	27.0±17.48	22.35±12.1	19.45±12.7	24.33±12.57	33.35±19.08	29.01±18.74	27.32±21.84	27.53±21.31	21.27±16.32	23.35±20.35

HCM: hypertrophic cardiomyopathy; LGE: late gadolinium enhancement.

* Total of 1200 segments analyzed – 16 American Heart Association segments for the 75 hypertrophic cardiomyopathy patients.

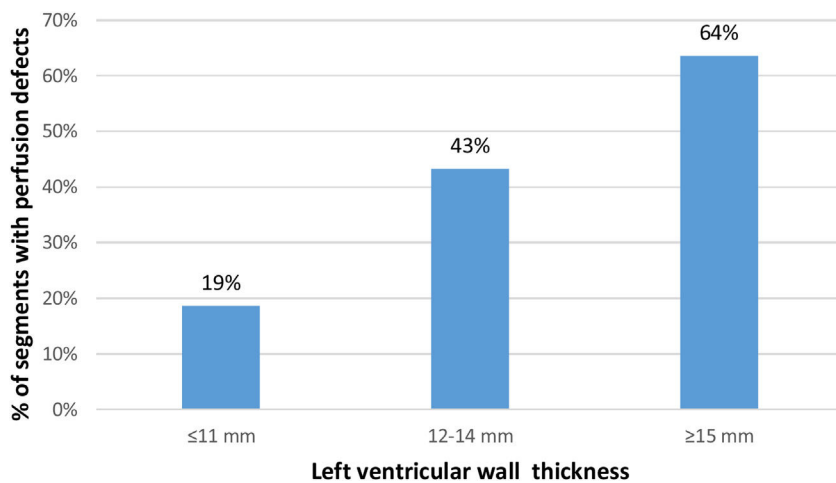


Figure 1 Left ventricular segments with perfusion defects (%) according to intervals of maximal wall thickness.

Among the 424 segments (35.3%) with a perfusion defect, 286 (23.8%) only had a defect in the endocardial layer and 138 (11.5%) in both endocardial and epicardial layers. Perfusion defects were present in 19% of non-hypertrophied segments and were more often detected in hypertrophied segments: in 43.3% of the segments with 12-14 mm and in 63.6% of the segments with ≥ 15 mm (Figure 1).

The distribution and prevalence of perfusion defects and LGE in each of the 16 AHA segments is displayed in Figure 2.

Coronary microvascular dysfunction and tissue characteristics

The results of univariable regression analysis for potential factors associated with T1 mapping, T2 mapping, LGE and ECV are presented in Supplementary Table 1. Subsequently, a multivariable regression analysis, adjusted for potential confounders, was performed (Table 2).

Perfusion defects were associated with changes in tissue characteristics, independently of LV wall thickness (Figure 3). Segments with perfusion defect had a higher native T1 than those without (β -estimate 30.28, 95% CI 24.60-35.96, $p<0.001$), as well as a significantly higher ECV (β -estimate 1.50, 95% CI 0.81-2.11, $p<0.001$). T2 values were also higher in segments with perfusion defect (β -estimate 0.73, 95% CI 0.32-1.14, $p<0.001$) (Table 2 and Figure 3).

Furthermore, regardless of the wall thickness, segments with a perfusion defect more frequently had LGE (OR 4.16, 95% CI 3.19-5.41, $p<0.001$) (Figure 2). Among the 424 segments with perfusion defect, 115 segments (27.1%) did not present LGE.

Besides perfusion defects, wall thickness and obstructive HCM were features associated with tissue abnormalities (Table 2).

Left ventricular myocardial deformation

Univariable regression analyses for longitudinal strain, radial strain and circumferential strain are shown in Supplementary Table 2 and the multivariable analyses are described below.

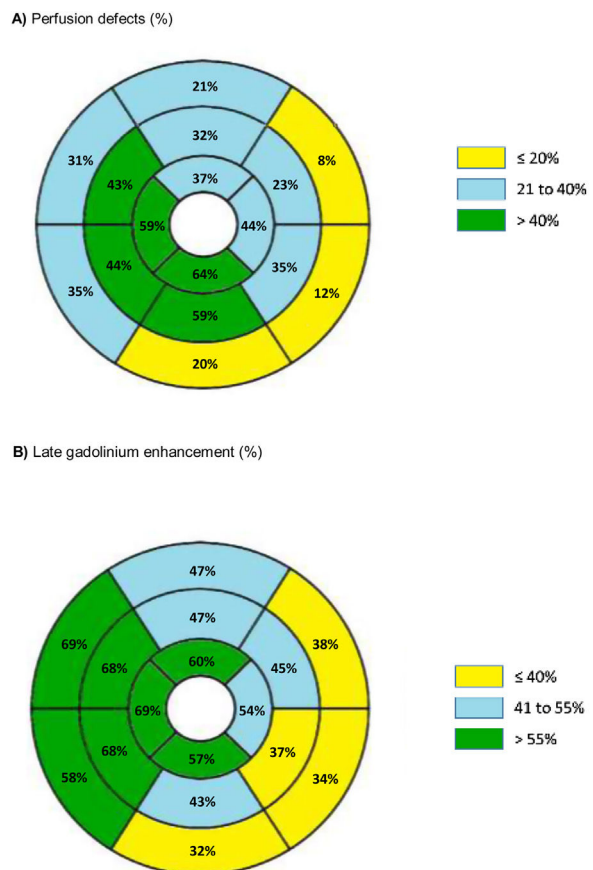


Figure 2 Ischemia (A) and late gadolinium enhancement (B) frequency in individual cardiac magnetic resonance segments
A) Perfusion defects (%).

Higher values of longitudinal strain (reflecting lower deformation) were found in segments with wall thickness ≥ 15 mm (β -estimate 2.28, 95% CI 0.87-3.69, $p=0.002$) compared with non-hypertrophied segments (Table 3). No association was found between perfusion defects and longitudinal strain in this segmental analysis. Higher values of circumferential strain (lower deformation) were found in

Table 2 Multivariable logistic and linear regression analyses for tissue characteristics.

Native T1 mapping			
Model	β-estimate	95% CI	p-value
Thickness 12-14 mm	16.69	9.29 to 24.08	<0.001
Thickness \geq 15 mm	38.09	31.58 to 44.60	<0.001
Perfusion defect	30.28	24.60 to 35.96	<0.001
LGE	32.04	26.61 to 37.47	<0.001
Diabetes	11.37	2.91 to 19.83	0.009
BMI $>$ 25 kg/m ²	11.37	3.74 to 18.98	0.004
Male gender	-15.52	-22.03 to -9.01	<0.001
Extracellular volume			
Model	β-estimate	95% CI	p-value
Thickness \geq 15 mm	2.40	1.60 to 3.10	<0.001
Perfusion defect	1.50	0.81 to 2.11	<0.001
LGE	2.92	2.32 to 3.50	<0.001
Diabetes mellitus	2.90	1.90 to 3.81	<0.001
Hypertension	1.50	0.70 to 2.20	<0.001
T2 mapping			
Model	β-estimate	95% CI	p-value
Perfusion defect	0.73	0.32 to 1.14	<0.001
LGE	1.06	0.67 to 1.45	<0.001
Obstructive HCM	1.17	0.73 to 1.61	<0.001
BMI $>$ 25 kg/m ²			0.001
Male gender	-0.50	-0.95 to -0.05	0.030
Late gadolinium enhancement			
Model	OR estimate	95% CI	p-value
Thickness 12-14 mm	2.66	1.92 to 3.68	<0.001
Thickness \geq 15 mm	9.02	6.42 to 12.67	<0.001
Perfusion defect	4.16	3.19 to 5.41	<0.001
Obstructive HCM	2.08	1.43 to 2.48	<0.001
Diabetes	1.82	1.26 to 2.63	0.001
BMI $>$ 25 kg/m ²	2.10	1.52 to 2.90	<0.001
Hypertension	1.65	1.23 to 2.16	<0.001

Reference categories: Wall thickness \leq 11 mm, non-obstructive HCM, absence of perfusion defect. p-values were obtained using a mixed effects regression models.

CI: confidence interval; HCM: hypertrophic cardiomyopathy; LGE: late gadolinium enhancement; OR: odds ratio.

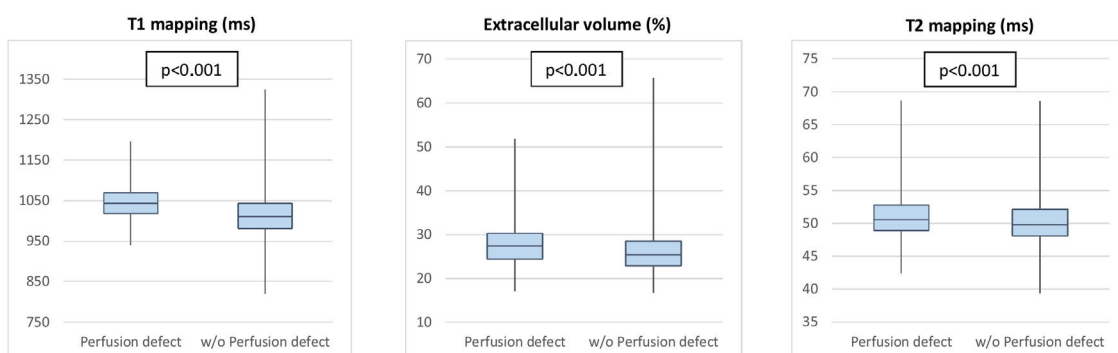
**Figure 3** Tissue characterization (T1 mapping, extracellular volume, T2 mapping) features, according to the presence or absence of perfusion defects.

Table 3 Multivariable linear regression analysis for left ventricular myocardial deformation parameters.

Longitudinal strain			
Model	β-estimate	95% CI	p-value
Thickness ≥ 15 mm	2.28	0.87 to 3.69	0.002
Obstructive HCM	2.62	1.32 to 3.92	<0.001
BMI > 25 kg/m ²	3.14	1.56 to 4.72	<0.001
Circumferential strain			
Model	β-estimate	95% CI	p-value
Thickness 12-4 mm	2.31	1.35 to 3.26	<0.001
Thickness ≥ 15 mm	5.14	4.32 to 5.97	<0.001
Perfusion defect	2.76	2.01 to 3.50	<0.001
LGE	2.30	1.57 to 3.02	<0.001
Obstructive HCM	1.56	0.75 to 2.37	<0.001
Diabetes	2.43	1.37 to 3.50	<0.001
Male gender	1.72	0.89 to 2.55	<0.001
Radial strain			
Model	β-estimate	95% CI	p-value
Thickness 12-14mm	-9.90	-13.19 to -6.59	<0.001
Thickness ≥ 15 mm	-19.78	-22.48 to -17.09	<0.001
Perfusion defect	-10.39	-12.83 to -7.95	<0.001
LGE	-9.84	-12.19 to -7.48	<0.001
Obstructive HCM	-4.84	-7.51 to -2.16	<0.001
Diabetes	-6.54	-10.07 to -3.00	0.027
BMI > 25 kg/m ²	-4.73	-7.94 to -1.52	0.004
Hypertension	-7.06	-9.82 to -4.29	<0.001
Male gender	-6.82	-9.55 to -4.09	<0.001

Reference categories: wall thickness ≤ 11 mm, non-obstructive HCM, absence of perfusion defect, female gender, BMI ≤ 25 kg/m². p-values were obtained by mixed effects regression models. BMI: body mass index; CI: confidence interval; LGE: late gadolinium enhancement; HCM: hypertrophic cardiomyopathy.

segments with wall thickness 12-14 mm (β -estimate 2.31, 95% CI 1.35-3.26, $p<0.001$), wall thickness ≥ 15 mm (β -estimate 5.14, 95% CI 4.32-5.97, $p<0.001$) versus segments with normal wall thickness, in segments with perfusion defect (β -estimate 2.76, 95% CI 2.01-3.50, $p<0.001$) and in segments with LGE (β -estimate 2.30, 95% CI 1.57-3.02, $p<0.001$). Lower radial strain values (reflecting lower myocardial deformation) were found in segments with wall thickness 12-14 mm (β -estimate -9.90, 95% CI -13.19--6.59, $p<0.001$) and wall thickness ≥ 15 mm (β -estimate -19.78, 95% CI -22.48--17.09, $p<0.001$) in contrast to non-hypertrophied segments, segments with perfusion defect (β -estimate -10.39, 95% CI -12.83--7.95, $p<0.001$) and with LGE (β -estimate -9.84, 95% CI -12.19--7.48, $p<0.001$) (Table 3).

No association was found between T1 and T2 mapping values, ECV and tissue tracking analysis.

Discussion

In patients with HCM, we performed segmental analysis and found an independent association between segmental ischemia and abnormal tissue characteristics. This association was noted between ischemia and tissue abnormalities

studied using native T1, ECV and T2 mapping, as well as replacement fibrosis studied using LGE. In this segmental analysis, CMD was further related to impaired circumferential strain and radial strain. Importantly, some of these associations were uncovered by the current segmental analysis but were not present in our previous global assessment of ischemia burden,²³ which might be explained by the inherent intra-individual phenotypic heterogeneity of LV segments in HCM.

To better appreciate the intrinsic characteristics of HCM even in segments without overt LV hypertrophy, we aimed to examine segments with normal wall thickness and segments with mild hypertrophy for the presence of ischemia and tissue abnormalities.

As expected, hypertrophied segments had more severe microvascular dysfunction, with segments ≥ 15 mm demonstrating a higher prevalence of perfusion defects. However, microvascular dysfunction is only partly explained by hypertrophy, since it was also found in 19% of non-hypertrophied segments, reflecting the existence of intrinsic structural and functional abnormalities of the small vessels.⁷⁻⁹ This is a similar finding to previously published works.^{10,25,30}

Notably, almost half of segments with mild hypertrophy had microvascular dysfunction. These findings confirm that segments with normal wall thickness and segments with mild

hypertrophy are also important contributors to the overall burden of ischemia in HCM.

Among the segments with perfusion defects, the subendocardium in isolation was involved in two-thirds. This is in keeping with previous results, including a multimodality study using invasive LV pressure measurements and noninvasive imaging with echocardiography, CMR and PET. This study demonstrated that the autoregulatory mechanisms of the microvasculature are insufficient during vasodilatory stress, leading to subendocardial ischemia, while the subepicardium was relatively spared.³¹

Impact of ischemia in tissue abnormalities

As a hallmark of the disease, severity of wall thickness was expectedly associated with tissue abnormalities. However, segments with only mild hypertrophy also showed the presence of increased T1 mapping and of LGE, displaying tissue abnormalities even in the absence of overt LV hypertrophy.

Regardless of the severity of hypertrophy, CMD was consistently related to tissue abnormalities in this study. Segments with perfusion defects were linked to both increased ECV and LGE, indicating the presence of both diffuse tissue abnormalities and replacement fibrosis.^{17,18} Hypertrophied myocytes are arranged in disarray, with increased extracellular matrix accumulation. While reduced ECV can be seen in cellular hypertrophy³² and in healthy athletes,³³ ECV has been demonstrated to be increased in HCM in the context of focal or diffuse fibrosis,³⁴ albeit with considerable heterogeneity among HCM patients.³² Moreover, while LGE may not accurately reveal the presence of abnormal tissue in the setting of less severe or more diffuse fibrosis, ECV has shown to be a surrogate for the presence of fibrosis in a significantly higher percentage of cardiac segments compared to LGE.³⁵

Histologically, the severity of the abnormalities in intramural small vessels was previously found to be co-localized with fibrotic scars.^{17,18} By CMR stress perfusion, higher ischemic burden and lower stress myocardial blood flow were found to be linked to the presence of LGE.^{25,36} This suggests that replacement fibrosis may be partially secondary to microvascular dysfunction and ischemia.^{30,37,38} However, while LGE burden is a recognized prognostic factor particularly in advanced stages, it is tempting to speculate that ECV may detect earlier pathophysiological changes in HCM. Similarly, CMD is a pathological feature that seems to have an impact from an early stage of the disease, and thus may be a useful marker of disease progression and prognosis.^{13,39}

Native T1 mapping reflects diffuse abnormalities in both the intracellular and extracellular spaces.⁴⁰ In HCM, native T1 may be affected by the intracellular compartment where altered calcium cycling and sarcomeric calcium sensitivity, disturbed biomechanical stress sensing and impaired cardiac energy homeostasis have been detected.⁴¹ In our cohort, higher native T1 levels correlated with myocardial ischemia. This finding suggests that CMD may be associated not only with increased diffuse fibrosis but also with intracellular compartment abnormalities.

T2-weighted imaging, a tissue characterization technique mainly used to identify edema, can be elevated in HCM,⁴² both in hypertrophied and non-hypertrophied

segments, despite normal wall thickness and preserved contractile function, which suggests that tissue abnormalities may precede morphological and functional remodeling in HCM.⁴³ Furthermore, higher T2 values were previously correlated with higher brain natriuretic peptide levels, higher LGE extension and nonsustained ventricular tachycardia and have, therefore, been suggested as a possible marker for arrhythmogenicity.⁴⁴ In our cohort, segments with higher T2 values were associated with greater LGE extent as well as with ischemia. To our knowledge, this is the first evidence of correlation between higher T2 and ischemia.

Impact of microvascular dysfunction on myocardial deformation

Speckle tracking parameters for systolic function are often impaired in HCM, such as longitudinal, circumferential and radial strain. Changes in these parameters vary widely between segments, reflecting the asymmetric nature of the disease. They are more prominent in segments with significant hypertrophy and fibrosis.⁴⁵⁻⁴⁷ In line with previous data,⁴⁸ and using a per-segment analysis, we found a relationship between wall thickness and LGE and impaired LV myocardial deformation parameters.

Furthermore, hypoperfused segments showed worse circumferential and radial strain, independently of wall thickness or fibrosis, which is a novel - although probably expected - finding.

As LV performance is determined by several factors other than ischemia, such as wall thickness and extent of replacement fibrosis, with considerable heterogeneity among patients and within the left ventricle,⁴⁶ in this study we did not find a correlation between impaired longitudinal strain and perfusion defects.

Limitations

One limitation of our study is the relatively small population. Six patients were in AF during the scan, which may have influenced parametric mapping values. CMR assessment of tissue characteristics was not validated with histological samples. Perfusion defects, a surrogate for myocardial ischemia, were assessed using a semiquantitative visual analysis of ischemia in 32 segments, as used in previous studies comparing stress CMR with invasive evaluation of fractional flow reserve.¹⁴ While the adopted method is readily available and easily applicable, it relies on visual assessment and the total of LV assessed is 96% (3% for each segment).

Conclusion

While perfusion defects were more prevalent in more hypertrophied segments, segments with normal wall thickness and mild hypertrophy accounted significantly for the overall burden of ischemia in HCM. The presence of microvascular dysfunction was associated with diffuse tissue abnormalities and replacement fibrosis. Segments with perfusion defect presented worse LV myocardial deformation assessed using radial and circumferential strain. Our findings suggest

that CMD is an important early pathophysiological feature, impacting on tissue abnormalities (including T1, ECV and T2 mapping) and LV performance on a per-segment basis, regardless of the severity of the hypertrophy, with significant intra-individual heterogeneity among LV segments. These findings highlight that symptoms in HCM may be attributable to CMD, which can be impactful even in patients with no significant hypertrophy.

These abnormalities merit further study and suggest that ischemia might be a useful and early imaging biomarker, which could potentially be used to help develop therapies that may change the progression of the disease and outcomes.

Conflicts of interest

The authors have no conflicts of interest to declare.

References

1. Elliott P, Anastasakis A, Borger M, et al. 2014 ESC guidelines on diagnosis and management of hypertrophic cardiomyopathy. *Eur Heart J.* 2015;121:7–57.
2. Bruder O, Wagner A, Jensen C, et al. Myocardial scar visualized by cardiovascular magnetic resonance imaging predicts major adverse events in patients with hypertrophic cardiomyopathy. *J Am Coll Cardiol.* 2010;56:875–87.
3. O'Hanlon R, Grasso A, Roughton M, et al. Prognostic significance of myocardial fibrosis in hypertrophic cardiomyopathy. *J Am Coll Cardiol.* 2010;56:867–74.
4. Adabag A, Maron B, Appelbaum E, et al. Occurrence and frequency of arrhythmias in hypertrophic cardiomyopathy in relation to delayed enhancement on cardiovascular magnetic resonance. *J Am Coll Cardiol.* 2008;51:1369–413.
5. Maron M, Appelbaum E, Harrigan C, et al. Clinical profile and significance of delayed enhancement in hypertrophic cardiomyopathy. *Circ Hear Fail.* 2008;1:184–91.
6. Chan R, Maron B, Olivotto I, et al. Prognostic value of quantitative contrast-enhanced cardiovascular magnetic resonance for the evaluation of sudden death risk in patients with hypertrophic cardiomyopathy. *Circulation.* 2014;130:484–549.
7. Basso C, Thiene G, Corrado D, et al. Hypertrophic cardiomyopathy and sudden death in the young: pathologic evidence of myocardial ischemia. *Hum Pathol.* 2000;31, <http://dx.doi.org/10.1053/hupa.2000.16659>.
8. O'Gorman D, Sheridan D. Abnormalities of the coronary circulation associated with left ventricular hypertrophy. *Clin Sci.* 1991;81:703–13.
9. Maron B, Wolfson J, Epstein S, et al. Intramural ("small vessel") coronary artery disease in hypertrophic cardiomyopathy. *J Am Coll Cardiol.* 1986;8:545–57.
10. Petersen S, Jerosch-Herold M, Hudsmith L, et al. Evidence for microvascular dysfunction in hypertrophic cardiomyopathy: new insights from multiparametric magnetic resonance imaging. *Circulation.* 2007;115:2418–25.
11. Barbosa A, Almeida J, Guerreiro C, et al. Late gadolinium enhancement location assessed by magnetic resonance and arrhythmogenic risk in hypertrophic cardiomyopathy. *Rev Port Cardiol.* 2020;39:615–21.
12. Scialgrà R, Passeri A, Bucerius J, et al. Clinical use of quantitative cardiac perfusion PET: rationale, modalities and possible indications. Position paper of the Cardiovascular Committee of the European Association of Nuclear Medicine (EANM). *Eur J Nucl Med Mol Imaging.* 2016;43, <http://dx.doi.org/10.1007/s00259-016-3317-5>.
13. Lorenzoni R, Gistri R, Cecchi F, et al. Coronary vasodilator reserve is impaired in patients with hypertrophic cardiomyopathy and left ventricular dysfunction. *Am Hear J.* 1998;136, [http://dx.doi.org/10.1016/S0002-8703\(98\)70152-8](http://dx.doi.org/10.1016/S0002-8703(98)70152-8).
14. Choudhury L, Rosen S, Patel D, et al. Coronary vasodilator reserve in primary and secondary left ventricular hypertrophy. A study with positron emission tomography. *Eur Hear J.* 1997;18:108–16.
15. Camici P, Chiriaci G, Lorenzoni R, et al. Coronary vasodilation is impaired in both hypertrophied and non-hypertrophied myocardium of patients with hypertrophic cardiomyopathy: a study with nitrogen-13 ammonia and positron emission tomography. *J Am Coll Cardiol.* 1991;17, [http://dx.doi.org/10.1016/0735-1097\(91\)90869-b](http://dx.doi.org/10.1016/0735-1097(91)90869-b).
16. Hughes R, Camaioni C, Augusto J, et al. Myocardial perfusion defects in hypertrophic cardiomyopathy mutation carriers. *J Am Heart Assoc.* 2021;10:e020227.
17. Moon J, Reed E, Sheppard M, et al. The histologic basis of late gadolinium enhancement cardiovascular magnetic resonance in hypertrophic cardiomyopathy. *J Am Coll Cardiol.* 2004;43:2260–4.
18. Galati G, Leone O, Pasquale F, et al. Histological and histometric characterization of myocardial fibrosis in end-stage hypertrophic cardiomyopathy: a clinical-pathological study of 30 explanted hearts. *Circ Hear Fail.* 2016;9, <http://dx.doi.org/10.1161/CIRCHEARTFAILURE.116.003090>.
19. Iles L, Ellims A, Llewellyn H, et al. Histological validation of cardiac magnetic resonance analysis of regional and diffuse interstitial myocardial fibrosis. *Eur Hear J Cardiovasc Imaging.* 2015;16, <http://dx.doi.org/10.1093/eihjci/jeu182>.
20. Moon J, Messroghli D, Kellman P, et al., Myocardial T1 mapping and extracellular volume quantification: a society for cardiovascular magnetic resonance (SCMR) and CMR working group of the European Society of Cardiology Consensus Statement. *J Cardiovasc Magn Reson.* 2013;15:92.
21. Frey N, Luedde M, Katus H. Mechanisms of disease: hypertrophic cardiomyopathy. *Nat Rev Cardiol.* 2011;9:91–100.
22. Todiere G, Pisciella L, Barison A, et al. Abnormal T2-STIR magnetic resonance in hypertrophic cardiomyopathy: a marker of advanced disease and electrical myocardial instability. *PLOS ONE.* 2014;9, <http://dx.doi.org/10.1371/journal.pone.0111366>.
23. Aguiar Rosa S, Thomas B, Fiarres A, et al. The impact of ischemia assessed by magnetic resonance on functional, arrhythmic and imaging features of hypertrophic cardiomyopathy. *Front Cardiovasc Med.* 2021;8, <http://dx.doi.org/10.3389/fcvm.2021.761860>.
24. Yin L, Xu HY, Zheng SS, et al. 3.0 T magnetic resonance myocardial perfusion imaging for semi-quantitative evaluation of coronary microvascular dysfunction in hypertrophic cardiomyopathy. *Int J Cardiovasc Imaging.* 2017;33:1949–59.
25. Camaioni C, Knott K, Augusto J, et al. Inline perfusion mapping provides insights into the disease mechanism in hypertrophic cardiomyopathy. *Heart.* 2020;106:824–82.
26. Bravo P, Zimmerman S, Luo H, et al. Relationship of delayed enhancement by magnetic resonance to myocardial perfusion by positron emission tomography in hypertrophic cardiomyopathy. *Circ Cardiovasc Imaging.* 2013;6:210–7.
27. Scialgrà R, Sotgia B, Olivotto I, et al. Relationship between atrial fibrillation and blunted hyperemic myocardial blood flow in patients with hypertrophic cardiomyopathy. *J Nucl Cardiol.* 2009;16:92–6.
28. Cecchi F, Sgalambro A, Baldi M, et al. Microvascular dysfunction, myocardial ischemia, and progression to heart failure in patients with hypertrophic cardiomyopathy. *J Cardiovasc Transl Res.* 2009;2:452–61.
29. Omens SR, Mital S, Burke MA, et al. 2020 AHA/ACC guideline for the diagnosis and treatment of patients

- with hypertrophic cardiomyopathy. *Circulation*. 2020;142:e558–631.
30. Das A, Kelly C, Teh I, et al. Phenotyping hypertrophic cardiomyopathy using cardiac diffusion magnetic resonance imaging: the relationship between microvascular dysfunction and microstructural changes. *Eur Hear J - Cardiovasc Imaging*. 2021, <http://dx.doi.org/10.1093/ehjci/jeab210>, jeab210.
 31. Knaapen P, Germans T, Camici P, et al. Determinants of coronary microvascular dysfunction in symptomatic hypertrophic cardiomyopathy. *Am J Physiol Hear Circ Physiol*. 2008;294:H98.
 32. Castelletti S, Menacho K, Davies R, et al. Hypertrophic cardiomyopathy: insights from extracellular volume mapping. *Eur J Prev Cardiol*. 2022;28:e39–41.
 33. McDiarmid A, Swobodan P, Erhayien B, et al. Athletic cardiac adaptation in males is a consequence of elevated myocyte mass. *Circ Cardiovasc Imaging*. 2016;9:e003579.
 34. Minegishi S, Kato S, Takase-Minegishi K, et al. Native T1 time and extracellular volume fraction in differentiation of normal myocardium from non-ischemic dilated and hypertrophic cardiomyopathy myocardium: a systematic review and meta-analysis. *Int J Cardiol Hear Vasc*. 2019;25:100422.
 35. Ali N, Behairy N, Kharabish A, et al. T1 mapping and extracellular volume application in hypertrophic cardiomyopathy. *Egypt J Radiol Nucl Med*. 2021;52:58.
 36. Villa A, Sammut E, Zarinabad N, et al. Microvascular ischemia in hypertrophic cardiomyopathy: new insights from high-resolution combined quantification of perfusion and late gadolinium enhancement. *J Cardiovasc Magn Reson*. 2016;14:1.
 37. Sotgia B, Sciagà R, Olivotto I, et al. Spatial relationship between coronary microvascular dysfunction and delayed contrast enhancement in patients with hypertrophic cardiomyopathy. *J Nucl Med*. 2008;49, <http://dx.doi.org/10.2967/jnumed.107.050138>.
 38. Aguiar Rosa S, Rocha Lopes L, Fiarresga A, et al. Coronary microvascular dysfunction in hypertrophic cardiomyopathy: pathophysiology, assessment, and clinical impact. *Microcirculation*. 2021;28:e12656.
 39. Shirani J, Pick R, Roberts W, et al. Morphology and significance of the left ventricular collagen network in young patients with hypertrophic cardiomyopathy and sudden cardiac death. *J Am Coll Cardiol*. 2000;35:36–44.
 40. Schelbert E, Messroghli D. State of the Art: clinical applications of cardiac T1 mapping. *Radiology*. 2016;278:658–76.
 41. Camici P, Olivotto I, Rimoldi O. The coronary circulation and blood flow in left ventricular hypertrophy. *J Mol Cell Cardiol*. 2012;52:857–64.
 42. Gastl M, Lachmann V, Christidi A, et al. Cardiac magnetic resonance T2 mapping and feature tracking in athlete's heart and HCM. *Eur Radiol*. 2020;31:2768–77.
 43. Huang L, Ran L, Zhao P, et al. MRI native T1 and T2 mapping of myocardial segments in hypertrophic cardiomyopathy: tissue remodeling manifested prior to structure changes. *Br J Radiol*. 2019;92:20190634.
 44. Baig M, Galazka P, Dakwar O, et al. Prevalence of myocardial edema with T2 mapping in hypertrophic cardiomyopathy. *J Am Coll Cardiol*. 2021;77 Suppl_1:1303.
 45. Urbano-Moral J, Rowin E, Maron M, et al. Investigation of global and regional myocardial mechanics with 3-dimensional speckle tracking echocardiography and relations to hypertrophy and fibrosis in hypertrophic cardiomyopathy. *Circ Cardiovasc Imaging*. 2014;7:11–9.
 46. Popović Z, Kwon D, Mishra M, et al. Association between regional ventricular function and myocardial fibrosis in hypertrophic cardiomyopathy assessed by speckle tracking echocardiography and delayed hyperenhancement magnetic resonance imaging. *J Am Soc Echocardiogr*. 2008;21:129.
 47. Barbosa A, Dias Ferreira N, Martins O'Neill C, et al. Impaired myocardial deformation assessed by cardiac magnetic resonance is associated with increased arrhythmic risk in hypertrophic cardiomyopathy. *Rev Esp Cardiol (Engl Ed)*. 2020, <http://dx.doi.org/10.1016/j.rec.2020.02.008>, S1885-5857.
 48. Valentim Gonçalves A, Aguiar Rosa S, Branco L, et al. Myocardial work is associated with significant left ventricular myocardial fibrosis in patients with hypertrophic cardiomyopathy. *Int J Cardiovasc Imaging*. 2021;2357, <http://dx.doi.org/10.1007/s10554-021-02186-3>.